

Spin-polarized transport through a single-level quantum dot in the Kondo regime

R. Świrkowicz¹, M. Wilczyński¹, and J. Barnaś^{2*}

¹*Faculty of Physics, Warsaw University of Technology, ul. Koszykowa 75, 00-662 Warszawa, Poland*

²*Department of Physics, Adam Mickiewicz University, ul. Umultowska 85, 61-614 Poznań, Poland; and Institute of Molecular Physics, Polish Academy of Sciences, ul. Smoluchowskiego 17, 60-179 Poznań, Poland*

(Dated: November 20, 2018)

Nonequilibrium electronic transport through a quantum dot coupled to ferromagnetic leads (electrodes) is studied theoretically by the nonequilibrium Green function technique. The system is described by the Anderson model with arbitrary correlation parameter U . Exchange interaction between the dot and ferromagnetic electrodes is taken into account *via* an effective molecular field. The following situations are analyzed numerically: (i) the dot is symmetrically coupled to two ferromagnetic leads, (ii) one of the two ferromagnetic leads is half-metallic with almost total spin polarization of electron states at the Fermi level, and (iii) one of the two electrodes is nonmagnetic whereas the other one is ferromagnetic. Generally, the Kondo peak in the density of states (DOS) becomes spin-split when the total exchange field acting on the dot is nonzero. The spin-splitting of the Kondo peak in DOS leads to splitting and suppression of the corresponding zero bias anomaly in the differential conductance.

PACS numbers: 75.20.Hr, 72.15.Qm, 72.25.-b, 73.23.Hk

I. INTRODUCTION

The Kondo phenomenon in electronic transport through artificial quantum dots (QDs) or single molecules attached to nonmagnetic leads was predicted theoretically more than a decade ago [1]. Owing to recent progress in nanotechnology, the phenomenon has been also observed experimentally [2, 3]. Several theoretical techniques have been developed to describe this effect [4, 5, 6, 7, 8, 9, 10, 11]. The description is usually simpler in the linear response regime, where equilibrium methods can be applied, but it becomes more complex when the system is driven out of equilibrium by an external bias voltage [7, 11, 12, 13, 14, 15]. One of the methods used to describe non-equilibrium Kondo effect is the non-equilibrium Green function technique [5, 16, 17]. To calculate density of states (DOS) and electric current one then needs the retarded/advanced as well as the lesser (correlation) Green functions. These can be derived within some approximation schemes.

It has been shown recently that the Kondo effect can also occur when replacing nonmagnetic leads by ferromagnetic ones [18, 19, 20, 21, 22], but ferromagnetism of the electrodes generally suppresses the effect – either partially or totally [19, 22]. However, in some peculiar situations the effect remains almost unchanged. Suppression of the Kondo anomaly is a consequence of an effective exchange field due to coupling between the dot and ferromagnetic electrodes. The exchange field gives rise to spin-splitting of the equilibrium Kondo peak in DOS, and the two components of the splitted peak move away from the Fermi level, which leads to suppression

of the Kondo anomaly in electrical conductance – similarly as an external magnetic field suppresses the effect in nonmagnetic systems. Such a suppression was studied recently by the Green function technique in the limit of infinite correlation parameter U [19], and was also confirmed by numerical renormalization group calculations [23, 24]. However, only QDs symmetrically coupled to two magnetic leads were studied up to now. The Kondo anomaly survives then in the antiparallel magnetic configuration and is significantly suppressed in the parallel one. Recent experimental observations on C_{60} molecules attached to ferromagnetic (Ni) electrodes support these general theoretical predictions [25].

Some features of the non-equilibrium Kondo phenomenon in QDs coupled to ferromagnetic leads have not been addressed yet. Therefore, in this paper we consider a more general situation. First of all, we consider the case when the two ferromagnetic electrodes are generally different. In other words, the dot is (spin-)asymmetrically coupled to the ferromagnetic leads. This leads to qualitatively new results. Second, we consider the case of arbitrary U instead of the limiting situation of infinite U studied in [19]. Third, we introduce an effective exchange field to describe the dot level renormalization.

We analyze in detail three different situations. In the first case the dot is coupled to two ferromagnetic leads, and the coupling is fully symmetric in the parallel magnetic configuration. We show that the equilibrium Kondo peak in DOS is then spin-split in the parallel configuration, whereas no splitting appears in the antiparallel one. The splitting, however, is significantly reduced for small values of the correlation parameter U . The corresponding zero-bias anomaly in conductance becomes split in the parallel configuration as well [19]. The second situation studied in this paper is the one with asymmetric coupling to two ferromagnetic leads. As a particular case we consider the situation when one of the ferromagnetic

*Electronic address: barnas@main.amu.edu.pl

electrodes is half metallic, with almost total spin polarization of electron states at the Fermi level. Such structures have been shown recently to have transport characteristics with typical diode-like behavior [26, 27]. Finally, we also analyze the case when one of the electrodes is nonmagnetic whereas the second one is ferromagnetic, and show that one ferromagnetic electrode is sufficient to generate spin-splitting of the Kondo anomaly.

The paper is organized as follows. The model and method are briefly described in Sections 2 and 3, respectively. Numerical results for the three different situations mentioned above are presented and discussed in Section 4. Summary and general conclusions are given in Section 5.

II. MODEL

We consider a single-level QD coupled to ferromagnetic metallic leads (electrodes) by tunnelling barriers. We restrict our considerations to collinear (parallel and antiparallel) magnetic configurations and assume that the axis z (spin quantization axis) points in the direction of the net spin of the left electrode (opposite to the corresponding magnetic moment). Antiparallel alignment is obtained by reversing magnetic moment of the right electrode. The whole system is then described by Hamiltonian of the general form

$$H = H_L + H_R + H_D + H_T. \quad (1)$$

The terms H_β describe here the left ($\beta = L$) and right ($\beta = R$) electrodes in the non-interacting quasi-particle approximation, $H_\beta = \sum_{k\sigma} \varepsilon_{k\beta\sigma} c_{k\beta\sigma}^\dagger c_{k\beta\sigma}$, where $\varepsilon_{k\beta\sigma}$ is the single-electron energy in the electrode β for the wave-number k and spin σ ($\sigma = \uparrow, \downarrow$), whereas $c_{k\beta\sigma}^\dagger$ and $c_{k\beta\sigma}$ are the corresponding creation and annihilation operators. The single-particle energy $\varepsilon_{k\beta\sigma}$ includes the electrostatic energy due to applied voltage, $\varepsilon_{k\beta\sigma} = \varepsilon_{k\beta\sigma}^0 + eU_e^\beta = \varepsilon_{k\beta\sigma}^0 + \mu_\beta$, where $\varepsilon_{k\beta\sigma}^0$ is the corresponding energy in the unbiased system, U_e^β is the electrostatic potential of the β -th electrode, e stands for the electron charge ($e < 0$), and μ_β is the chemical potential of the β -th electrode (the energy is measured from the Fermi level of unbiased system). Electron spin projection on the global quantization axis is denoted as \uparrow for $s_z = 1/2$ and \downarrow and for $s_z = -1/2$. On the other hand, spin projection on the local quantization axis (local spin polarization in the ferromagnetic material) will be denoted as $+$ for spin-majority and $-$ for spin-minority electrons, respectively. When local and global quantization axes coincide, then \uparrow is equivalent to $+$ and \downarrow is equivalent to $-$. (Note, that the local quantization axis in the ferromagnet is opposite to the local magnetization.)

The term H_D in Eq.(1) describes the quantum dot and takes the form

$$H_D = \sum_\sigma \epsilon_\sigma d_\sigma^\dagger d_\sigma + U d_\uparrow^\dagger d_\uparrow d_\downarrow^\dagger d_\downarrow, \quad (2)$$

where ϵ_σ denotes energy of the dot level (spin-dependent in a general case), U denotes the electron correlation parameter, whereas d_σ^\dagger and d_σ are the creation and annihilation operators for electrons on the dot. The level energy ϵ_σ includes the electrostatic energy due to applied voltage, $\epsilon_\sigma = \epsilon_{0\sigma} + eU_e^d$, where U_e^d is the electrostatic potential of the dot, and $\epsilon_{0\sigma}$ is the level energy at zero bias.

The electrostatic potential U_e^d of the dot will be determined fully self-consistently from the following capacitance model [28, 29]:

$$e \left(\sum_\sigma n_\sigma - \sum_\sigma n_{0\sigma} \right) = C_L(U_e^d - U_e^L) + C_R(U_e^d - U_e^R), \quad (3)$$

where n_σ and $n_{0\sigma}$ are the dot occupation numbers $\langle d_\sigma^\dagger d_\sigma \rangle$ calculated for a given bias and for zero bias, respectively, whereas C_L and C_R denote the capacitances of the left and right tunnel junctions. Self-consistent determination of the dot electrostatic potential makes the description gauge invariant. This is particularly important for strongly asymmetric systems.

The last term, H_T , in Eq.(1) describes tunnelling processes between the dot and electrodes and is of the form

$$H_T = \sum_{k\beta\sigma} V_{k\beta\sigma}^* c_{k\beta\sigma}^\dagger d_\sigma + \text{h.c.}, \quad (4)$$

where $V_{k\beta\sigma}$ are the components of the tunnelling matrix, and h.c. stands for the Hermitian conjugate term. Hamiltonian (4) includes only spin-conserving tunnelling processes.

III. THEORETICAL FORMULATION

Electric current flowing from the β -th lead to the quantum dot in a nonequilibrium situation is determined by the retarded (advanced) $G_\sigma^{r(a)}$ and correlation (lesser) $G_\sigma^<$ Green functions of the dot (calculated in the presence of coupling to the electrodes), and is given by the formula [30]

$$I_\sigma^\beta = \frac{ie}{\hbar} \int \frac{dE}{2\pi} \Gamma_\sigma^\beta(E) \{ G_\sigma^<(E) + f_\beta(E) [G_\sigma^r(E) - G_\sigma^a(E)] \}, \quad (5)$$

where $f_\beta(E)$ is the Fermi distribution function for the β -th electrode. The retarded (advanced) Green functions can be calculated from the corresponding equation of motion. The key difficulty is with calculating the lesser Green function $G_\sigma^<(E)$.

In a recent paper [31] we applied the equation of motion method to derive both $G_\sigma^r(E)$ and $G_\sigma^<(E)$ Green functions within the same approximation scheme [32]. However, the approximations for the lesser Green function $G_\sigma^<(E)$ do not conserve charge current in asymmetric systems. Therefore, in the following we assume

constant (independent of energy) coupling parameters, $\Gamma_\sigma^\beta(E) = 2\pi \sum_k V_{k\beta\sigma} V_{k\beta\sigma}^* \delta(E - \varepsilon_{k\beta\sigma}) = \Gamma_\sigma^\beta$. As pointed out in Refs [33, 34], it is then sufficient to determine $\int (dE/2\pi) G_\sigma^<(E)$, while knowledge of the exact form of $G_\sigma^<(E)$ is not necessary. Current conservation condition allows then to express the above integral by an integral including retarded and advanced Green functions only, which in turn allows to rewrite the current formula in the commonly used form,

$$I_\sigma = \frac{ie}{\hbar} \int \frac{dE}{2\pi} \frac{\Gamma_\sigma^L \Gamma_\sigma^R}{\Gamma_\sigma^L + \Gamma_\sigma^R} [G_\sigma^r(E) - G_\sigma^a(E)][f_L(E) - f_R(E)]. \quad (6)$$

Similarly, the occupation numbers, $n_\sigma = \langle d_\sigma^+ d_\sigma \rangle$, are then given by the formula

$$\begin{aligned} n_\sigma &= -i \int \frac{dE}{2\pi} G_\sigma^<(E) \\ &= i \int \frac{dE}{2\pi} \frac{\Gamma_\sigma^L f_L(E) + \Gamma_\sigma^R f_R(E)}{\Gamma_\sigma^L + \Gamma_\sigma^R} [G_\sigma^r(E) - G_\sigma^a(E)]. \quad (7) \end{aligned}$$

In the following the parameters Γ_σ^β will be used to parameterize strength of the coupling between the dot and leads. It is convenient to introduce the spin polarization factors p_β defined as $p_\beta = (\Gamma_+^\beta - \Gamma_-^\beta)/(\Gamma_+^\beta + \Gamma_-^\beta)$, where Γ_+^β and Γ_-^β are the coupling parameters for spin-majority and spin-minority electrons in the lead β , respectively. Accordingly, one may write $\Gamma_+^\beta = (1 + p_\beta)\Gamma^\beta$ and $\Gamma_-^\beta = (1 - p_\beta)\Gamma^\beta$, with $\Gamma^\beta = (\Gamma_+^\beta + \Gamma_-^\beta)/2$.

The retarded (advanced) Green function $G_\sigma^{r(a)}$ of the dot can be calculated only approximately, for instance by the equation of motion method. In the approximations introduced by Meir et al [5] one finds

$$G_\sigma^r(E) = \frac{E - \epsilon_\sigma - U(1 - n_{-\sigma})}{[E - \epsilon_\sigma - \Sigma_\sigma^r(E)](E - \epsilon_\sigma - U) - Un_{-\sigma}\Sigma_\sigma^r(E)}, \quad (8)$$

where Σ_σ^r is the corresponding self energy,

$$\Sigma_\sigma^r(E) = \Sigma_{0\sigma}^r(E) + U \frac{(E - \epsilon_\sigma)n_{-\sigma}\Sigma_{03\sigma}^r(E) - L_{0\sigma}\Sigma_{01\sigma}^r(E)}{L_{0\sigma}(E)[L_{0\sigma}(E) - \Sigma_{03\sigma}^r(E)]}, \quad (9)$$

with $L_{0\sigma} = E - \epsilon_\sigma - U(1 - n_{-\sigma})$, and $\Sigma_{01\sigma}^r(E)$ and $\Sigma_{03\sigma}^r(E)$ defined as

$$\Sigma_{01\sigma}^r(E) = n_{-\sigma}\Sigma_{0\sigma}^r(E) + \Sigma_{1\sigma}^r(E), \quad (10)$$

$$\Sigma_{03\sigma}^r(E) = \Sigma_{0\sigma}^r(E) + \Sigma_{3\sigma}^r(E). \quad (11)$$

The self energies $\Sigma_{0\sigma}^r(E)$, $\Sigma_{1\sigma}^r(E)$, and $\Sigma_{3\sigma}^r(E)$ are defined as

$$\Sigma_{0\sigma}^r(E) = \sum_{\beta=L,R} \Sigma_{0\sigma}^{\beta r}(E) = \sum_{\beta=L,R} \sum_k |V_{k\beta\sigma}|^2 \frac{1}{E - \varepsilon_{k\beta\sigma} + i0^+}$$

$$= \sum_{\beta=LR} \int \frac{d\varepsilon}{2\pi} \frac{\Gamma_\sigma^\beta}{E - \varepsilon} - i \frac{\Gamma_\sigma^\beta}{2} \quad (12)$$

and

$$\begin{aligned} \Sigma_{i\sigma}^r(E) &= \sum_{\beta=LR} \int \frac{d\varepsilon}{2\pi} A_i \Gamma_{-\sigma}^\beta \left[-\frac{1}{\varepsilon - E - \epsilon_{-\sigma} + \epsilon_\sigma - i\hbar/\tau_{-\sigma}} \right. \\ &\quad \left. + \frac{1}{\varepsilon + E - \epsilon_{-\sigma} - \epsilon_\sigma - U - i\hbar/\tau_{-\sigma}} \right], \quad (13) \end{aligned}$$

(for $i=1,3$), where $A_1 = f(\varepsilon)$, $A_3 = 1$, and $\tau_{-\sigma}$ is the relaxation time of the intermediate states [5]. This relaxation time is spin dependent and in the low-temperature limit is given by the formula [5]

$$\begin{aligned} \frac{1}{\tau_\sigma} &= \frac{1}{2\pi\hbar} \sum_{\beta,\beta'} \sum_{\sigma'} \Gamma_\sigma^\beta \Gamma_{\sigma'}^{\beta'} \Theta(\mu_{\beta'} - \mu_\beta + \epsilon_\sigma - \epsilon_{\sigma'}) \\ &\quad \times \frac{\mu_{\beta'} - \mu_\beta + \epsilon_\sigma - \epsilon_{\sigma'}}{(\mu_\beta - \epsilon_\sigma)(\mu_{\beta'} - \epsilon_{\sigma'})}, \quad (14) \end{aligned}$$

where $\Theta(x) = 0$ for $x < 0$ and $\Theta(x) = 1$ otherwise.

In the limit of infinite U the Green function (8) reduces to the well known form,

$$G_\sigma^r(E) = \frac{1 - n_{-\sigma}}{E - \epsilon_\sigma - \Sigma_{0\sigma}^r(E) - \Sigma_{1\sigma}^r(E)}, \quad (15)$$

where $\Sigma_{0\sigma}^r(E)$ is given by Eq.(12) and $\Sigma_{1\sigma}^r(E)$ by

$$\Sigma_{1\sigma}^r(E) = \sum_{\beta=L,R} \Sigma_{1\sigma}^{\beta r}(E)$$

$$\equiv \sum_{\beta=L,R} \int \frac{d\varepsilon}{2\pi} \frac{f_\beta(\varepsilon)\Gamma_{-\sigma}^\beta}{-\varepsilon + E + \epsilon_{-\sigma} - \epsilon_\sigma + i\hbar/\tau_{-\sigma}}, \quad (16)$$

and τ_σ defined by Eq.(14).

The above derived Green functions are sufficient to describe qualitatively basic features of the Kondo phenomenon in QDs attached to nonmagnetic leads [5]. However, they are not sufficient to describe properly the Kondo phenomenon when the quantum dot is attached to ferromagnetic leads. The key feature of the system, which is not sufficiently taken into account is the splitting of the dot level due to spin dependent tunneling processes [19]. The most natural way would rely on an extension of the Green function calculations by going beyond the approximations used to derive Eq.(8). This, however, leads to cumbersome expressions. To avoid this, one may treat the problem approximately by introducing 'by hand' the level splitting to the formalism described above. One way to achieve such an objective was proposed in Ref.[19] for the limit of infinite U , where the

bare dot level ϵ_σ in $\Sigma_{1\sigma}^r(E)$ and $\Sigma_{0\sigma}^r(E)$ was replaced by the renormalized energy $\tilde{\epsilon}_\sigma$ calculated in a self-consistent way. Such a renormalization works well in the limit of infinite U . It is however not clear how to extend it to the general case of arbitrary U . Therefore, we decided to include the level splitting *via* an effective exchange field. The exchange-induced spin-splitting of the level is particularly important for the self-energies $\Sigma_{1\sigma}^r(E)$ and $\Sigma_{3\sigma}^r(E)$, so we replace the bare energy levels in the self-energies $\Sigma_{1\sigma}^r(E)$ and $\Sigma_{3\sigma}^r(E)$ by the corresponding renormalized levels $\tilde{\epsilon}_\sigma = \epsilon_\sigma \pm g\mu_B B_{\text{ex}}/2$, with the exchange field calculated from the formula

$$B_{\text{ex}} = \frac{1}{g\mu_B} \sum_{\beta=R,L} \text{Re} \int \frac{d\epsilon}{2\pi} f_\beta(\epsilon) \times \left[\Gamma_\uparrow^\beta \left(\frac{1}{\epsilon - \epsilon_\uparrow - i\hbar/\tau_\uparrow} - \frac{1}{\epsilon - \epsilon_\uparrow - U - i\hbar/\tau_\uparrow} \right) - \Gamma_\downarrow^\beta \left(\frac{1}{\epsilon - \epsilon_\downarrow - i\hbar/\tau_\downarrow} - \frac{1}{\epsilon - \epsilon_\downarrow - U - i\hbar/\tau_\downarrow} \right) \right]. \quad (17)$$

When the bare dot level and spin relaxation time are independent of the spin orientation, $\epsilon_\uparrow = \epsilon_\downarrow = \epsilon$ and $\tau_\uparrow = \tau_\downarrow = \tau$, the formula (14) acquires the form [35]

$$B_{\text{ex}} = \frac{1}{g\mu_B} \sum_{\beta=R,L} \text{Re} \int \frac{d\epsilon}{2\pi} f_\beta(\epsilon) \times \left(\Gamma_\uparrow^\beta - \Gamma_\downarrow^\beta \right) \left(\frac{1}{\epsilon - \epsilon - i\hbar/\tau} - \frac{1}{\epsilon - \epsilon - U - i\hbar/\tau} \right). \quad (18)$$

To some extent such an approach is similar to that used in Ref.[19], and both approaches give similar results in the limit of large U . This follows from the fact that the expression (17) for exchange field is basically the expression for the self energy $\Sigma_{i\sigma}^r$ (see Eq.(13) for $i = 1$ and $E = \epsilon_\sigma$). However, the approach based on the exchange field allows to handle easily also the general case of finite U .

IV. NUMERICAL RESULTS

Now, we apply the above described formalism to the Kondo problem in a QD coupled to ferromagnetic leads. In the numerical calculations described below the energy is measured in the units of D , where $D = \bar{D}/50$ and \bar{D} is the electron band width. For simplicity, the electron band in the leads is assumed to be independent of the spin orientation and extends from $-25D$ below the Fermi level (bottom band edge) up to $25D$ above the Fermi level (top band edge). The energy integrals will be cut off at $E = \pm 25D$, i.e., will be limited to the electron band. Thus, the influence of ferromagnetic electrodes

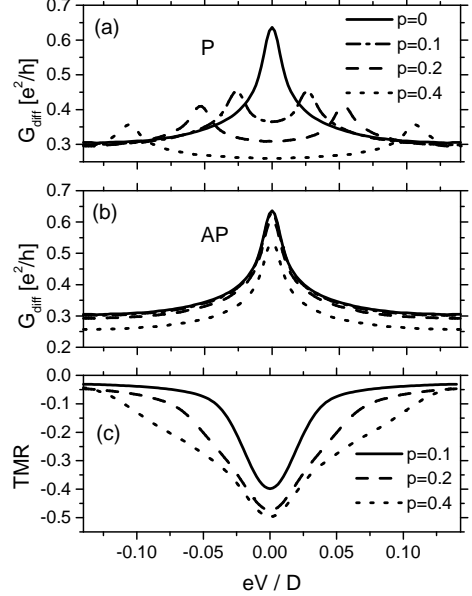


FIG. 1: Bias dependence of the differential conductance in the parallel (a) and antiparallel (b) configurations, and the corresponding TMR (c) for indicated four values of the lead polarization $p_L = p_R = p$ ($p = 0$ corresponds to nonmagnetic leads so the corresponding TMR vanishes and is not shown in part (c)). The parameters assumed for numerical calculations are: $kT/D = 0.001$, $\Gamma^L/D = \Gamma^R/D = 0.1$, $\epsilon_{0\uparrow}/D = \epsilon_{0\downarrow}/D = \epsilon_0/D = -0.35$, $U/D = 500$, and $(e^2/C_L)/D = (e^2/C_R)/D = 0.33$.

is included only *via* the spin asymmetry of the coupling parameters Γ_σ^L and Γ_σ^R . Apart from this, in all numerical calculations we assumed $kT/D = 0.001$ and $\epsilon_{0\uparrow}/D = \epsilon_{0\downarrow}/D = \epsilon_0/D = -0.35$.

For positive (negative) bias we assume the electrostatic potential of the left (right) electrode equal to zero. In other words, electrochemical potential of the drain electrode is assumed to be zero while of the source electrode is shifted up by $|eV|$. In the following the bias is described by the corresponding electrostatic energy eV . Note that positive eV corresponds to negative bias due to negative electron charge ($e < 0$).

A. QD coupled to two similar ferromagnetic leads

Consider first the situation when both electrodes are made of the same ferromagnetic metal, and the coupling of the dot to both leads is symmetrical (in the parallel configuration). For numerical calculations we assumed $\Gamma_+^L/D = \Gamma_+^R/D = 0.12$ for spin-majority electrons and $\Gamma_-^L/D = \Gamma_-^R/D = 0.08$ for spin-minority ones, which corresponds to the spin polarization factor $p_L = p_R = p = 0.2$, and $\Gamma^L/D = \Gamma^R/D = 0.1$.

It was shown in Ref.[19] that ferromagnetism of the electrodes leads to spin splitting of the Kondo peak in the density of states (DOS) in the parallel configuration,

whereas no splitting occurs for the antiparallel orientation. Such a behavior of DOS has a significant influence on the transport properties. First of all, the Kondo peak in DOS leads to zero bias anomaly in the differential conductance $G_{diff} = \partial I / \partial V$. This anomaly is particularly interesting in the parallel configuration, where the spin splitting of the Kondo peak in DOS leads to splitting of the differential conductance, as shown in Fig.1(a) for four different values of the electrode spin polarization factor p and for large U . For $p = 0$ there is only a single peak centered at zero bias. When the polarization factor becomes nonzero, the peak becomes split into two components located symmetrically on both sides of the original peak, with the corresponding intensities significantly suppressed. The splitting of the Kondo anomaly increases with increasing p . Moreover, height of the two components of the Kondo anomaly decreases with increasing p . On the other hand, in the antiparallel configuration there is no splitting of the Kondo peak in the density of states and consequently also no splitting of the Kondo anomaly in the differential conductance (see Fig.1(b)). For all polarization values, the anomaly is similar to that in the case of QDs coupled to nonmagnetic leads. However, intensity of the Kondo anomaly decreases with increasing polarization. Difference between conductance in the antiparallel and parallel configurations gives rise to the TMR effect which may be described quantitatively by the ratio $(I^P - I^{AP})/I^{AP}$, where I^P and I^{AP} denote the current flowing through the system in the parallel and antiparallel configurations at the same bias, respectively. The associated TMR effect is displayed in Fig.1(c). One finds negative values of the TMR ratio, which is a consequence of the spin-splitting of the Kondo peak in the parallel configuration and absence of such a splitting for antiparallel alignment. It is worth to note, that in the absence of the Kondo anomaly the TMR effect would be positive.

The Kondo anomaly in transport characteristics shown in Fig.1 was calculated for the limit of large U . In Fig.2 we show similar characteristics as in Fig.1, but for different values of the correlation parameter U and a constant value of the polarization factor p . The splitting of the Kondo anomaly in the parallel configuration and intensity of the peaks (Fig.2(a)) decrease with decreasing U . In the antiparallel configuration there is no splitting of the Kondo anomaly, but intensity of the Kondo peak decreases with decreasing U . The associated TMR effect is shown in Fig.2(c). The effect is negative in a certain bias range around the zero bias limit, but absolute magnitude of the effect becomes smaller for smaller values of U . For large bias there is a transition from negative to positive TMR with decreasing U .

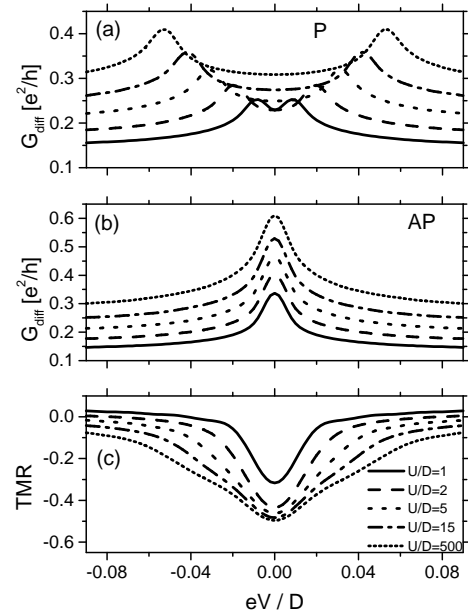


FIG. 2: Bias dependence of differential conductance in the parallel (a) and antiparallel (b) configurations, and the corresponding TMR (c) calculated for indicated values of the correlation parameter U and for $p = 0.2$. The other parameters are as in Fig.1.

B. QD coupled to one ferromagnetic and one half-metallic leads

Assume now that one of the electrodes (say the left one) is made of a 3-d ferromagnetic metal, the second (right) one is half-metallic, and the total coupling to the latter electrode is much smaller than to the former one. This is reflected in the spin asymmetry of the bare coupling constants, for which we assume $\Gamma_+^L/D = 0.28$ and $\Gamma_-^L/D = 0.12$ for the left electrode, and $\Gamma_+^R/D = 0.04$ and $\Gamma_-^R/D = 0.0002$ for the right one. These parameters correspond to $p_L = 0.4$, $p_R = 0.99$, $\Gamma^L/D = 0.2$, and $\Gamma^R/D \approx 0.02$. Thus, the spin asymmetry of the coupling to the right electrode is much larger than to the left one. In Fig.3 we show DOS in the parallel (left column) and antiparallel (right column) magnetic configurations, calculated for vanishing as well as for positive and negative bias voltages. Consider now the main features of the spectra in more details, and let us begin with the parallel configuration (left column in Fig.3).

At $V = 0$ the Kondo peak in DOS is spin-split, and the intensity of spin-down peak is relatively large, whereas that of the spin-up peak is much smaller. The asymmetry in peak intensities is a consequence of the spin asymmetry in the coupling of the dot to metallic electrodes – this coupling is larger for spin-up electron, which determines height of the Kondo peak for spin-down electrons. When a bias voltage is applied, each of the two Kondo peaks generally becomes additionally split into two components.

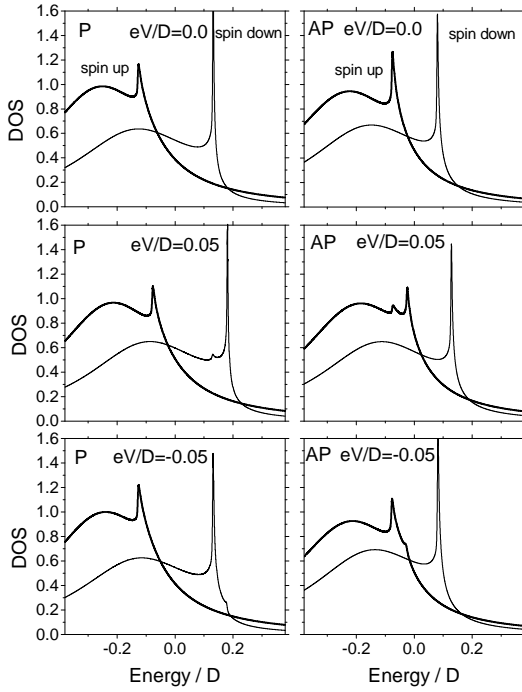


FIG. 3: DOS for spin-up (thick lines) and spin-down (thin lines) electron states on the dot in the parallel (left column) and antiparallel (right column) magnetic configurations, calculated for three indicated voltages and for $\Gamma_+^L/D = 0.28$, $\Gamma_-^L/D = 0.12$, $\Gamma_+^R/D = 0.04$, $\Gamma_-^R/D = 0.0002$, $U/D = 500$, $(e^2/C_L)/D = (e^2/C_R)/D = 10$. The other parameters are as in Fig.1.

One of them (the one associated with the coupling to the source electrode) moves up in energy, whereas position of the second one (the one associated with the drain electrode) remains unchanged. This is because we assumed that the electrochemical potential of the source electrode shifts up by $|eV|$, while of the drain electrode is independent of the voltage. For $eV > 0$ (negative bias), the splitting of the large-intensity (spin-down) peak is clearly visible, although one component of the splitted peak is relatively small. This is just the component associated with the coupling of the dot to the right electrode in the spin-up channel. Since this coupling is relatively small, the corresponding intensity is also small. The second component, in turn, is much larger because it is associated with the coupling to the left electrode in the spin-up channel, which is the dominant coupling in the system considered. Splitting of the low-intensity (spin-up) peak is not resolved. Intensity of the component associated with the coupling to the right electrode in the spin-down channel practically vanishes because this coupling is negligible in the case considered. For $eV < 0$ (positive bias), the situation is changed. Now the electrochemical potential of the left electrode is independent of the bias. Consequently, intensity of the components whose position is independent of energy is significantly larger than intensity of the other components (the ones associated

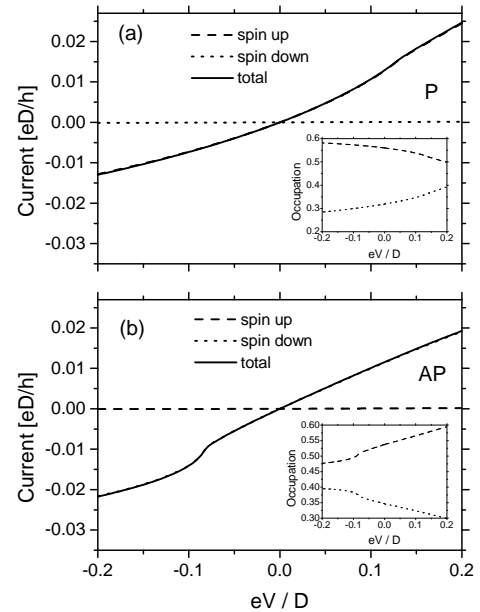


FIG. 4: Current-voltage characteristics in the parallel (a) and antiparallel (b) configurations, calculated for the parameters as in Fig.3. Current in the spin-down (spin-up) channel in the parallel (antiparallel) configuration almost vanishes so the total current flows in the spin-up (spin-down) channel (the curves presenting the total and spin-up (spin-down) currents are not resolved. The insets show the corresponding occupation numbers. The parameters as in Fig.3

with the right electrode). As before, the component associated with the coupling to the right electrode in the spin-down channel is not resolved.

Consider now the antiparallel configuration (right column in Fig.3), when magnetic moment of the right electrode is reversed. There is a nonzero spin splitting of the Kondo peak at equilibrium, contrary to the case of symmetric coupling to the magnetic electrodes, where the spin splitting in the antiparallel configuration vanishes [19]. Apart from this, the situation is qualitatively similar to the one for parallel configuration. The main difference is that now the bias-induced splitting of the large-intensity peak is not resolved, whereas splitting of the low-intensity peak is resolved.

As in the case of symmetrical coupling described above, the Kondo peaks in DOS give rise to anomalous behavior of the corresponding transport characteristics. Due to the splitting of the equilibrium Kondo peak, the anomaly in DOS does not contribute to transport in the small bias regime. The Kondo peaks enter the 'tunnelling window' at a certain bias, which leads to an enhanced conductance. Such an enhancement is clearly visible in the current-voltage characteristics shown in Fig.4 for both parallel (a) and antiparallel (b) configurations (solid lines), where for negative values of eV the enhancement is quite significant, but it is less pronounced for $eV > 0$. This asymmetry is due to the difference in intensities of

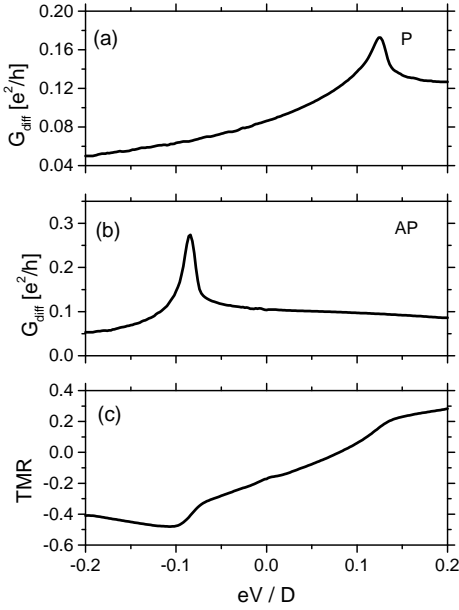


FIG. 5: Bias dependence of the differential conductance in the parallel (a) and antiparallel (b) configurations and the corresponding TMR (c), calculated for the same parameters as in Fig.3.

the corresponding Kondo peaks that enter the 'tunnelling window'.

The differential conductance in the Kondo regime is shown in Fig.5 for parallel (a) and antiparallel (b) magnetic configurations. In the parallel configuration the Kondo anomaly occurs in the spin-up channel and for $eV > 0$ only. This may be easily understood by considering the relevant DOS (see Fig.3, left column). For $eV > 0$ only the Kondo peak in spin-up DOS can enter the tunnelling window created by the bias. For $eV < 0$, on the other hand, the Kondo peak in spin-down DOS can enter the tunneling window. However, the spin down channel is almost non-conducting, so the corresponding peak in the differential conductance is suppressed. In the antiparallel configuration the Kondo peak in differential conductance occurs for $eV < 0$ only. This can be accounted for by taking into account behavior of the Kondo peaks in DOS shown in Fig.3 (right column), and the fact that now the spin-up channel is non-conducting. For $eV > 0$ only the Kondo peak in the spin-up DOS can enter the tunneling window, whereas for $eV < 0$ this is the Kondo peak in spin-down DOS (of large intensity).

The corresponding TMR is shown in Fig.5(c). It is interesting to note that TMR is highly asymmetric with respect to the bias reversal. It becomes positive for eV exceeding a certain positive value, and negative below this voltage. This is a consequence of the fact that for positive eV the Kondo peak in differential conductance is clearly visible in the parallel configuration (see Fig.5(a)), whereas for $eV < 0$ the Kondo peak occurs in the antiparallel configuration (see Fig.5(b)). Such a behavior of the

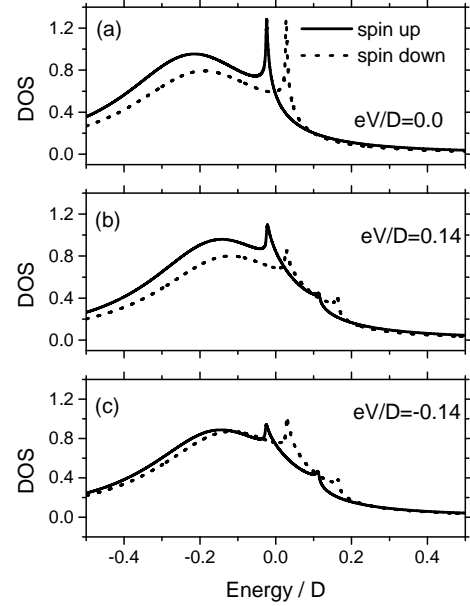


FIG. 6: DOS for spin-up (solid lines) and spin-down (dotted lines) electron states of the dot, calculated for three different voltages, and for $\Gamma_+^L/D = 0.12$, $\Gamma_-^L/D = 0.08$, $\Gamma_+^R/D = \Gamma_-^R/D = 0.1$, $U/D = 500$, and $(e^2/C_L)/D = (e^2/C_R)/D = 0.33$. The other parameters are as in Fig.1.

conductance and also TMR may be interesting from the point of view of applications in mesoscopic diodes.

C. QD coupled to one ferromagnetic and one nonmagnetic leads

A specific example of asymmetric systems is the case where one electrode is ferromagnetic (typical ferromagnetic 3d metal) whereas the second one is nonmagnetic. For numerical calculations we assumed $\Gamma_+^L/D = 0.12$, $\Gamma_-^L/D = 0.08$ for the left (magnetic) electrode, and $\Gamma_+^R/D = \Gamma_-^R/D = 0.1$ for the right (nonmagnetic) one, which corresponds to $p_L = 0.2$, $p_R = 0$, and $\Gamma^L/D = \Gamma^R/D = 0.1$. As in the other asymmetrical situations studied in this paper, the equilibrium Kondo peak in DOS becomes spin-split. When a bias voltage is applied, each component becomes additionally split, as shown in Fig.6. Variation of the spectra with bias voltage can be accounted for in a similar way as in the case of the dot coupled asymmetrically to two ferromagnetic electrodes. The only difference is that now all components of the peaks are clearly resolved. This is because all coupling constants are now of comparable magnitude.

The corresponding differential conductance is shown in Fig.7. Due to the spin splitting of the Kondo peak in DOS, the Kondo anomaly in the conductance becomes split as well, as clearly seen in Fig.7. However, the splitting is asymmetric with respect to the bias reversal. Thus, there is no need to have two ferromagnetic elec-

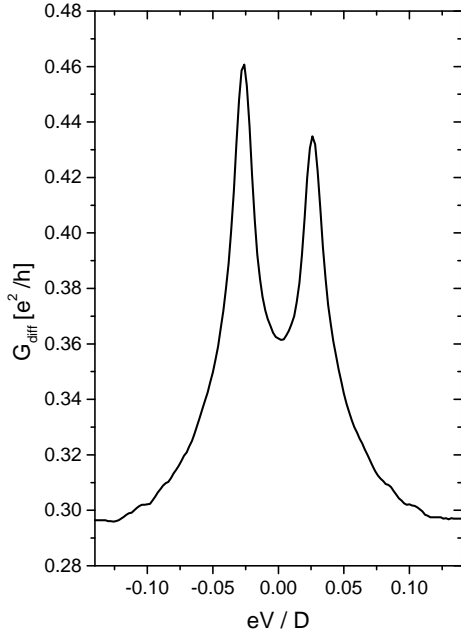


FIG. 7: Bias dependence of the differential conductance, calculated for the parameters as in Fig.6.

trodes to observe splitting of the Kondo anomaly, but it is sufficient when only one lead is ferromagnetic.

V. SUMMARY AND CONCLUSIONS

In this paper we considered the Kondo problem in quantum dots coupled symmetrically and asymmetrically to ferromagnetic leads. As a specific example of asymmetrical systems, we considered the case when one electrode is ferromagnetic, whereas the second one is nonmagnetic.

We showed that ferromagnetism of the leads gives rise to a splitting of the equilibrium Kondo peak in DOS for all asymmetrical situations. This generally takes place for both magnetic configurations when the two electrodes are different. The splitting in both configurations also occurs when both magnetic electrodes are of the same material, but the corresponding coupling strengths to the dot are different. Indeed, such a splitting in parallel and also antiparallel configurations was recently observed experimentally [25]. When similar electrodes are symmetrically coupled to the dot, the splitting occurs only in the parallel configuration. An interesting conclusion from the experimental point of view is that the splitting also occurs in the case when one electrode is nonmagnetic.

The spin-splitting of DOS can lead to characteristic splitting of the zero bias anomaly in electrical conductance. This in turn can lead to negative (inverse) tunnel magnetoresistance effect. In highly asymmetrical systems TMR can change sign when bias voltage is reversed.

Acknowledgments

The work was supported by the State Committee for Scientific Research through the Research Project PBZ/KBN/044/P03/2001 and 4 T11F 014 24.

[1] L. I. Glazman and M. E. Raikh, JETP Lett. **47**, 452 (1988); T. K. Ng and P. A. Lee, Phys. Rev. Lett. **61**, 1768 (1988).

[2] S.M. Cronenwett, T.H. Oosterkamp, and L.P. Kouwenhoven, Science **281**, 540 (1998); S. Sasaki, S.De Franceschi, J.M. Elzerman, W.G. van der Wiel, M. Eto, S. Tarucha, and L.P. Kouwenhoven, Nature (London) **405**, 764 (2000).

[3] J. Gores, D. Goldhaber-Gordon, S. Heemeyer, M.A. Kastner, H. Shtrikman, D. Mahalu, and U. Meirav, Phys. Rev. B **62**, 2188 (2000).

[4] S. Hershfield, J.H. Davies, and J.W. Wilkins, Phys. Rev. Lett. **67**, 3720 (1991).

[5] Y. Meir, N. S. Wingreen, and P. A. Lee, Phys. Rev. Lett. **70**, 2601 (1993).

[6] A. Levy-Yeyati, A. Martin-Rodero, and F. Flores, Phys. Rev. Lett. **71**, 2991 (1993); A. Levy-Yeyati, F. Flores, and A. Martin-Rodero, Phys. Rev. Lett. **83**, 600 (1999).

[7] N. S. Wingreen and Y. Meir, Phys. Rev. B **49**, 11 040 (1994).

[8] K. Kang and B.I. Min, Phys. Rev. B **52**, 10 689 (1995).

[9] J.J. Palacios, L. Liu, and D. Yoshioka, Phys. Rev. B **55**, 15 735 (1997).

[10] H. Schöller and J. König, Phys. Rev. Lett. **84**, 3686 (2000).

[11] M. Krawiec and K.I. Wysokiński, Phys. Rev. B **66**, 165408 (2002).

[12] T. A. Costi, Phys. Rev. Lett. **85**, 1504 (2000); Phys. Rev. B **64**, 241310 (2001).

[13] J. E. Moore, X-G. Wen, Phys. Rev. Lett. **85**, 1722 (2000).

[14] A. Kaminski, Yu.V Nazarov, and L.I. Glazman, Phys. Rev. B **62**, 8154 (2000).

[15] Y.W. Lee and Y.L. Lee, cond-mat/0105009 (2001).

[16] G. Czycholl, Phys. Rev. B **31**, 2867 (1985).

[17] H. Haug, and A-P. Jauho, Quantum Kinetics in Transport and Optics of Semiconductors, Springer Verlag, Berlin 1996.

[18] N. Sergueev, Q.F. Sun, H. Guo, B. G. Wang, and J. Wang, Phys. Rev. B **65**, 165303 (2002).

[19] J. Martinek, Y. Utsumi, H. Imamura, J. Barnaś, S. Maekawa, J. König, G. Schön, Phys. Rev. Lett. **91**, 127203 (2003).

[20] R. Lü and Z.R. Liu, cond-mat/0210350 (2002).

[21] B.R. Bułka and S. Lipiński, Phys. Rev. B **67**, 024404 (2003).

[22] R. Lopez and D. Sanchez, Phys. Rev. Lett. **90**, 116602 (2003).

[23] M.S. Choi, D. Sanchez, and R. Lopez, Phys. Rev. Lett. **92**, 056601 (2004).

[24] J. Martinek, M. Sindel, L. Borda, J. Barnaś, J. König, G. Schön, and J. von Delft, Phys. Rev. Lett. **91**, 247202 (2003).

[25] A.N. Pasupathy, L.C. Bialczak, J. Martinek, J.E. Grose, L.A.K. Donev, P.L. McEuen, and D.C. Ralph, Science **306**, 86 (2004).

[26] W. Rudzinski and J. Barnaś, Phys. Rev. B **69**, 085318 (2001).

[27] R.Świrkowicz, J. Barnaś, and M. Wilczyński, W. Rudzinski, V.D. Dugaev, J. Magn. Magn. Materials **272-276**, 1959 (2004).

[28] B. Wang, J. Wang, and H. Guo, J. Appl. Phys. **86**, 5094 (1999).

[29] R.Świrkowicz, J. Barnaś, and M. Wilczyński, J. Phys.: Condens. Matter **14**, 2011 (2002).

[30] A.P. Jauho, N.S. Wingreen, and Y. Meir, Phys. Rev. B **50**, 5528 (1994).

[31] R.Świrkowicz, J. Barnaś, and M. Wilczyński, Phys. Rev. B **68**, 195318 (2003).

[32] C. Niu, D.L. Lin, and T.H. Lin, J. Phys.: Condens. Matter **11**, 1511 (1999).

[33] K. Kang, Phys. Rev. B **57**, 11891 (1998).

[34] Q.-F. Sun and H. Guo, Phys. Rev. B **66**, 155308 (2002).

[35] M. Braun, J. König, J. Martinek, cond-mat/0404455.